Charge Inversion by Flexible Polyelectrolytes on Flat Surfaces from Self-Consistent Field Calculations

Qiang Wang†

Department of Chemical and Biological Engineering, Colorado State University, Fort Collins, Colorado 80523-1370

Received May 8, 2005; Revised Manuscript Received August 16, 2005

ABSTRACT: We have applied a continuum self-consistent field (SCF) theory to flexible polyelectrolytes on flat surfaces either uncharged or carrying charges opposite to the polyelectrolytes. We examined in detail the effects of various parameters on the polyelectrolyte adsorption and surface charge compensation by the adsorbed polyelectrolytes. The ground-state dominance approximation (GSDA) was used to explore the large parameter space involved, including the charge distribution and degree of ionization of the polyelectrolytes, surface charge density, short-range (non-Coulombic) surface−polymer interactions, solvent quality, and bulk polymer and salt concentrations. The numerical results under GSDA were also compared with full SCF calculations to examine the effects of molecular weight of the polyelectrolytes. Strong charge inversion is found for relatively long polyelectrolytes on oppositely charged, attractive surfaces in poor solvent at high salt concentrations. At the mean-field level, the adsorption behavior of polyelectrolytes at high salt concentrations can be understood by that of neutral polymers in good solvent.

1. Introduction

Theoretical study on polyelectrolyte adsorption has been carried out for about 30 years by now.[1,2] In this paper, we limit our discussion to equilibrium behavior of (untethered) flexible polyelectrolyte chains on flat and homogeneous surfaces. Two types of charge distribution on the chain are considered: In the case of "smeared" charge distribution, each polymer segment carries the same amount of charge; this is a model for strongly dissociating polyelectrolytes. In the case of "annealed" charge distribution, each polymer segment has the same probability of carrying a charge; this is a model for weakly dissociating polyelectrolytes. The early work of Hesselink assumed a step-function for the polymer segmental density profile in the adsorbed layer.[3,4] A better approach is to determine the profile without such a priori assumption; this leads to the self-consistent field (SCF) theory. Both lattice and continuum SCF theories have been used to study polyelectrolytes on or between flat surfaces. These are mean-field approaches, where the only variation in the system is along the direction perpendicular to the surface(s); the polymer chains are also modeled as intrinsically flexible (in addition to electrostatic stiffening effects).

Van der Schee and co-workers first extended the lattice SCF theory developed by Scheutjens and Fleer for neutral polymers[5,6] to the adsorption of polyelectrolytes having smeared charge distribution, where a uniform dielectric constant was used.[7,8] Due to some computational problem, most of their results were actually obtained based on an extension of Roe's theory.[9] Evers et al. extended this formalism further to the adsorption of polyelectrolytes having annealed charge distribution, and considered the case of position-dependent dielectric constant, which was taken as a linear combination (weighted by volume fractions) of those of pure polymer and solvent.[10] Using a multi-Stern-layer model, Böhmer et al. considered the finite volume of ions, which was set to be the same as that of the solvent molecules and polymer segments, and also included non-Coulombic interactions between ions and other species (including surface sites), which were described by the Flory−Huggins χ parameters.[11] These authors extended the theory of Scheutjens and Fleer,[5,6,12,13] and studied polyelectrolytes confined between two parallel surfaces.[11] Their formalism was used by van de Steeg et al., who studied in detail the effects of added salt on the adsorption of polyelectrolytes having smeared charge distribution, and they classified two regimes: the screening-enhanced regime where the adsorbed amount of polymers increases with increasing salt concentration and the screening-reduced regime where the opposite occurs.[14] Also using this formalism for polyelectrolytes having smeared charge distribution, Dahlgren and Leermakers examined the depletion zones (where the polymer segmental density is lower than that in the bulk) and the polydispersity effects on polyelectrolyte adsorption.[15] Linse systematically investigated the effects of various parameters in this formalism on the adsorption of weakly charged (and strongly dissociating) polyelectrolytes in a Θ-solvent.[16] On the basis of the lattice SCF theory, Fleer proposed an analytical "one-layer" model for adsorption of polyelectrolytes in dilute solutions of a good solvent on uncharged surfaces; good agreement with the numerical SCF results was obtained for highly charged polyelectrolytes.[17] In all the above studies, either a constant charge density or a constant electrostatic potential was used for the surface(s); this is in general not the case in experimental systems. Vermeer et al. introduced a dissociation equilibrium for surface sites, so that the charges carried by the surface can be controlled by solution pH.[18] In addition to this, Shubin and Linse used the site-binding model to account for the binding equilibrium between dissociated surface sites and cationic species (salt cations and dissociated polymer segments) in the first layer closest to the surface.[19]

The lattice SCF studies have greatly furthered our understanding on the behavior of polyelectrolytes on/between flat surfaces. The use of a underlying lattice,

† E-mail: q.wang@colostate.edu.

10.1021/ma050960b CCC: $30.25
Published on Web 09/21/2005

however, is an artifact that reduces the numerical accuracy in these calculations. This also makes it difficult to deal with the cases where the polymer segments, solvent molecules, and ions have different sizes. We therefore choose the continuum SCF theory. The governing equations in most previous mean-field studies in continuum[20−37] can be derived from our SCF equations presented in section 2 under various approximations. The ground-state dominance approximation (GSDA) has been commonly used to derive or solve the governing equations in these studies, with a few exceptions.[21−23,31,32] In addition, we note that, under GSDA, Joanny combined the scaling arguments for the electrostatic blob model with mean-field equations to study the polyelectrolyte adsorption in Θ-solvent.[38] A similar method was also used by Dobrynin, who studied the effects of solvent quality on polyelectrolyte adsorption.[39] Also under GSDA, Huang and Ruckenstein included explicitly the short-range (van der Waals) interactions between the surface and polymers in their governing equations (not through boundary conditions as shown below).[40] Through various analytical and numerical results, these continuum mean-field studies have provided us with important insights on polyelectrolytes on/between flat surfaces.

Recent study on polyelectrolyte adsorption has focused on the surface charge overcompensation (or charge inversion) by the adsorbed polyelectrolytes[37−39,41−46] due to its essential role in the polyelectrolyte layer-by-layer assembly process.[47−49] This phenomenon has been observed in experiments.[50−56] Here we define r as the ratio of the compensated surface charge (by the adsorbed polyelectrolytes) to the surface charge (including signs). In lattice SCF calculations, although only slight charge inversion ($r \approx 0$) was reported in earlier work,[11,14,16,18] Shubin and Linse reported strong charge inversion ($r < -1$) for polyelectrolytes with a small degree of ionization (0.034) on an attractive (through non-Coulombic interactions with the polymers) surface at high salt concentrations in Θ-solvent.[19] By analytically solving the mean-field equations, Joanny predicted full/strong charge inversion ($r \leq -1$) for indifferent/attractive surfaces at high salt concentrations in Θ-solvent.[38] His results, however, were questioned very recently by Shafir and Andelman, who numerically solved the same equations without the approximations made by Joanny; they found only moderate charge inversion ($-1 < r < 0$) for attractive surfaces at high salt concentrations in Θ-solvent.[37]

In this work, we present numerical results of the continuum SCF theory for flexible polyelectrolytes on flat surfaces. Our theoretical formalism and numerical methods are presented in section 2. In section 3, we examine in detail the effects of various parameters on the surface charge compensation by the adsorbed polyelectrolytes, including the charge distribution and degree of ionization of the polyelectrolytes, surface charge density, short-range (non-Coulombic) surface−polymer interactions, solvent quality, and bulk polymer and salt concentrations; GSDA is used to explore the large parameter space involved. Strong charge inversion is found for polyelectrolytes on oppositely charged, indifferent or attractive surfaces in poor solvent at high salt concentrations. In section 4, we follow the work of Joanny[38] and analytically solve the mean-field equations under GSDA; this allows us to understand the adsorption behavior of polyelectrolytes at high salt concentrations from that of neutral polymers in good solvent. The analytical results are also quantitatively compared with the numerical results to assess its applicability. In section 5, we compare the numerical results under GSDA with full SCF calculations to examine the effects of molecular weight of the polyelectrolytes; the strong charge inversion found at high salt concentrations is retained by relatively long polyelectrolytes. The last section is devoted to conclusions.

2. Theoretical Formalism

The general formalism of the continuum SCF theory for polyelectrolyte systems has been derived in refs 57 and 58. In this paper, we consider a system of charged homopolymers A with N_A segments on each chain in a solution of small-molecule solvent S. We assume that both polymer segments and solvent molecules have the same density ρ_0, and ignore the volume of small ions. We also assume that all ions carrying the same type of charge are identical, and denote cations by + and anions by −. Integer variables $v_+ > 0$, $v_- < 0$, and v_A are used to denote the increments of unit charge e carried by cations, anions, and polymer segments, respectively; without loss of generality, we set $v_A \leq 0$ hereafter. The system is in contact with a flat and homogeneous surface at $x = 0$; we assume that the system becomes effectively invariant at $x = L \gg 0$, where it is in contact with a bulk solution. The surface is either uncharged or positively charged. We assume that the system is invariant in the directions parallel to the surface, and only consider variations along the direction perpendicular to the surface (denoted by x).

2.1. Self-Consistent Field Equations. As in our previous work,[58] we include the following contribution to the Hamiltonian of the system: chain connectivity (treated with the Gaussian chain model), short-range (e.g., van der Waals) interactions between polymer segments and solvent molecules (modeled with the Flory−Huggins χ parameter), and the Coulombic interactions between all charges in the system (excluding the surface charges, which are considered later through boundary conditions). We then perform the Hubbard−Stratonovich transformation that introduces into the canonical partition function of the system the electrostatic potential $\psi(x)$ (in units of k_BT/e, where k_B is the Boltzmann constant and T the absolute temperature), a conjugate field $\omega_j(x)$ for each species j (=A, S, +, −), and a pressure field that imposes the incompressibility constraint everywhere in the system (note that all these fields are pure imaginary in our notation). Finally, the following set of SCF equations can be obtained under the saddle-point approximation

$$\phi_A(x) = \frac{\bar{\phi}_A N}{Q_A N_A} \int_0^{N_A/N} \mathrm{d}s\, q(x, s) q\left(x, \frac{N_A}{N} - s\right) \quad (1)$$

$$\omega_S(x) = \omega_A(x) + \chi N[2\phi_A(x) - 1] \quad (2)$$

$$F_1(x) \equiv \phi_A(x) + \frac{\bar{\phi}_S}{Q_S} \exp\left[-\frac{\omega_S(x)}{N}\right] - 1 = 0 \quad (3)$$

$$F_2(x) \equiv -\phi_A(x)\frac{\mathrm{d}g(x)}{\mathrm{d}\psi(x)} + \frac{v_+\bar{\phi}_+}{Q_+} \exp[-v_+\psi(x)] + \frac{v_-\bar{\phi}_-}{Q_-} \exp[-v_-\psi(x)] + \frac{\epsilon}{N}\frac{\mathrm{d}^2\psi(x)}{\mathrm{d}x^2} = 0 \quad (4)$$

where $\phi_A(x)$ denotes the normalized (by ρ_0) polymer segmental density field, which is constrained to the corresponding microscopic density by $\omega_A(x)$; $\bar{\phi}_A \equiv n_A N_A/(\rho_0 V)$ and $\bar{\phi}_M \equiv n_M/(\rho_0 V)$, where n_j is the number of molecules of species j in the system, V is the volume of the system, and M represents only the small-molecule species (i.e., S, +, and −); N is an (arbitrary) chain length chosen for the normalization discussed below; $q(x, s)$ corresponds to the probability of finding the end-segment of an A polymer of length sN at x, and it satisfies the modified diffusion equation

$$\frac{\partial q}{\partial s} = \frac{\partial^2 q}{\partial x^2} - [\omega_A(x) - Ng(x)]q \tag{5}$$

with the initial condition $q(x, s = 0) = 1$, where $s \in [0, N_A/N]$ is a variable along the chain contour; $g(x) \equiv -p\upsilon_A\psi(x)$ for the smeared charge distribution where each polymer segment carries charge $p\upsilon_A e$, and $g(x) \equiv \ln[1 - p + p \exp(-\upsilon_A\psi(x))]$ for the annealed charge distribution where each segment has a probability p of carrying charge $\upsilon_A e$. The single-chain/particle partition functions are defined as

$$Q_A \equiv \frac{1}{l}\int_0^l \mathrm{d}x\, q\left(x, \frac{N_A}{N}\right) \tag{6}$$

$$Q_S \equiv \frac{1}{l}\int_0^l \mathrm{d}x \exp\left[-\frac{\omega_S(x)}{N}\right] \tag{7}$$

$$Q_\pm \equiv \frac{1}{l}\int_0^l \mathrm{d}x \exp[-\upsilon_\pm \psi(x)] \tag{8}$$

where $l \equiv L/R_g$, $R_g \equiv a\sqrt{N/6}$, and a denotes the statistical segment length of polymers; ϵ is the dielectric constant, which is assumed to be uniform for $x \geq 0$. Note that to obtain the above equations we have made the following normalization: $x/R_g \to x$ and $3k_BT\epsilon/(2\pi\rho_0 e^2 a^2) \to \epsilon$ (where ϵ before the normalization is in units of $4\pi\epsilon_0$ with $\epsilon_0 = 8.854 \times 10^{-12}$ (A·s)^2/(J·m) being the permittivity of vacuum). Once the SCF equations are solved, the mean-field free energy (of mixing) per polymer segment or solvent molecule can be calculated as (in units of k_BT)

$$f = \frac{1}{l}\int_0^l \mathrm{d}x\left[\chi[1-\phi_A(x)]^2 - \frac{\omega_A(x)}{N} - \frac{\epsilon}{2N}\left(\frac{\mathrm{d}\psi}{\mathrm{d}x}\right)^2\right] - \frac{\bar{\phi}_A}{N_A}\ln\frac{Q_A}{\bar{\phi}_A} - \sum_M \bar{\phi}_M \ln\frac{Q_M}{\bar{\phi}_M} \tag{9}$$

Readers are referred to ref 58 for details on the above derivation. Finally, the incompressibility and the charge neutrality constraints on the whole system give

$$\bar{\phi}_S = 1 - \bar{\phi}_A$$

$$\upsilon_A p\bar{\phi}_A + \upsilon_+\bar{\phi}_+ + \upsilon_-\bar{\phi}_- + \frac{\sigma_{SF}}{l\sqrt{N}} = 0 \tag{10}$$

where the normalized surface charge density $\sigma_{SF} \equiv \sigma_0\sqrt{6}/(\rho_0 a)$, and σ_0 denotes the number of surface charges (in units of e) per unit area. We set $\sigma_{SF} \geq 0$ in this paper.

2.2. Boundary Conditions and Numerical Solution. At $x = 0$, we use the following boundary condition for $q(x, s)$: $[q - d\ (\partial q/\partial x)]|_{x=0} = 0$, where d^{-1} is proportional to the short-range (van der Waals) interactions between the surface and polymers. For surfaces attracting the polymers, $d^{-1} < 0$, and vice versa. The $d^{-1} = 0$ case is referred to as an indifferent surface, which corresponds to the boundary condition of $(\partial q/\partial x)|_{x=0} = 0$. The limit of $d^{-1} \to \infty$ is referred to as a nonadsorbing surface, which corresponds to the boundary condition of $q(x = 0, s) = 0$.[59] On the other hand, the surface can be held either at a constant electrostatic potential, which gives $\psi(x = 0) = \psi_{SF}$ (where the surface charge density is solved from the SCF equations), or at a constant surface charge density, which gives $(\mathrm{d}\psi/\mathrm{d}x)|_{x=0} = -\sigma_{SF}\sqrt{N}/\epsilon$ (where the surface electrostatic potential is solved); note that there is no difference between the two solutions for the corresponding cases.

At $x = l$, we use $(\partial q/\partial x)|_{x=l} = 0$ and $(\mathrm{d}\psi/\mathrm{d}x)|_{x=l} = 0$ as boundary conditions. We set the salt concentration $c_{s,b}$ (normalized by ρ_0) and the polymer segmental density $\phi_{A,b}$ in the bulk solution. We also use the bulk solution as the reference state for the electrostatic potential where we set $\psi = 0$; the Poisson−Boltzmann distribution of ions (refer to the second and third terms on the left-hand-side of eq 4) therefore gives

$$\frac{\bar{\phi}_+}{Q_+} = c_{s,b} - \frac{\upsilon_A p\phi_{A,b}}{\upsilon_+}$$

$$\frac{\bar{\phi}_-}{Q_-} = -\frac{\upsilon_+ c_{s,b}}{\upsilon_-}$$

where we have assumed that one salt molecule generates one cation. This effectively couples our system with the bulk solution for ions. To couple our system with the bulk solution for polyelectrolytes, we solve for $\bar{\phi}_A$ such that

$$F_3 \equiv \phi_A(l) - \phi_{A,b} = 0 \tag{11}$$

In general, we solve the modified diffusion equation by the Douglas scheme,[60] except for the case of indifferent surfaces where a pseudo-spectral method[61] with fast cosine transforms is used. The Douglas scheme is a finite-difference method superior to the commonly used Crank−Nicolson scheme in that it provides higher accuracy in the spatial domain with little extra work,[60] while the pseudo-spectral method has even higher accuracy in both the spatial and temporal (s) domains[61] (but is limited to certain boundary conditions). In both methods, the temporal domain $[0, N_A/N]$ is discretized (uniformly) into nN_A/N subintervals (where N is chosen such that nN_A/N is an integer). The SCF equations are solved in real space. The spatial domain $[0, l]$ is discretized (uniformly) at $m + 1$ nodes; we denote the position of node i by $x_i = il/m$, where $i = 0, ..., m$. We choose $\mathbf{X} \equiv \{\{\omega_A(x_i)\}, \{\psi(x_i)\}, \bar{\phi}_A\}$ as independent variables (σ_{SF}, instead of $\psi(x_0)$, is chosen for cases of constant surface electrostatic potential), and $\mathbf{F} \equiv \{\{F_1(x_i)\}, \{F_2(x_i)\}, F_3\} = 0$ as corresponding equations.[62] Second-order-accurate finite differences are used to numerically evaluate the spatial derivatives of $\psi(x)$, i.e., $(\mathrm{d}\psi/\mathrm{d}x)|_{x=x_i} = [\psi(x_{i+1}) - \psi(x_{i-1})]m/(2l)$ and $(\mathrm{d}^2\psi/\mathrm{d}x^2)|_{x=x_i} = [\psi(x_{i+1}) - 2\psi(x_i) + \psi(x_{i-1})]m^2/l^2$, where $\psi(x_{m+1}) = \psi(x_{m-1})$ and $\psi(x_{-1}) = \psi(x_1) + 2l\sqrt{N}\sigma_{SF}/(m\epsilon)$, consistent with the boundary conditions. A composite Simpson's rule is used to evaluate all integrals.

As noted in ref 58, $\{\omega_A(x_i)\}$ in the SCF solution can be uniformly shifted by an arbitrary constant; we

therefore set $Q_S = \bar{\phi}_S$ to obtain unique $\{\omega_A(x_i)\}$. The Broyden's method combined with a globally convergent strategy[63] is used to solve the set of nonlinear equations $\mathbf{F}(\mathbf{X}) = \mathbf{0}$, which provides fast convergence and high accuracy. In this work, the maximum absolute value of the residual errors of these equations is less than 10^{-10}.

In addition to the residual errors of $\mathbf{F}(\mathbf{X})$, there are other numerical errors introduced by using *finite* values of m, n, and l. We choose l to be large enough so that both $|\phi_A(l) - \phi_{A,b}|$ and $|\psi(l)|$ are less than 10^{-10}. Our values of n are on the order of 10^3-10^4, with larger n used for larger m or N_A. Because of the presence of the surface, the numerical accuracy is in general dictated by the discretization of the spatial domain; large values of m are needed to resolve the sharp variations near the surface. We use the following practical criterion to choose m: the absolute value of the difference between Q_S calculated according to $Q_S = 1 - \bar{\phi}_A$ and that from eq 7 is less than 10^{-10}; this typically requires m be on the order of 10^3.

2.3. Ground-State Dominance Approximation. The $q(x, s)$ in eq 5 can be expanded as $q(x, s) = \sum_{k=0}^{\infty} \exp(-\omega_k s) q_k(x)$, where ω_k and $q_k(x)$ are the eigenvalues and eigenfunctions of $-d^2/dx^2 + \omega_A(x) - Ng(x)$, respectively. For an infinitely long chain ($N_A \to \infty$) in the "bound" state where the differences between the smallest eigenvalue ω_0 and the others are finite, the ground-state dominance approximation can be used to truncate this expansion after the leading term.[64] This reduces eq 1 to $\phi_A(x) = \exp(-\omega_0 N_A/N) q_0^2(x) \bar{\phi}_A/Q_A$ and eq 5 to $d^2q_0/dx^2 = [\omega_A(x) - Ng(x) - \omega_0] q_0(x)$, from which one obtains

$$F_4(x) \equiv \frac{d^2}{dx^2}\sqrt{\phi_A(x)} - [\omega_A(x) - Ng(x) - \omega_0]\sqrt{\phi_A(x)} = 0 \quad (12)$$

The SCF equations can therefore be reduced to two coupled ordinary differential equations (ODEs), eqs 12 and 4, for $\sqrt{\phi_A(x)}$ and $\psi(x)$; $\omega_A(x)$ in eq 12 is calculated as

$$\omega_A(x) = \chi N[1 - 2\phi_A(x)] - N \ln[1 - \phi_A(x)] \quad (13)$$

where we have set $Q_S = 1 - \bar{\phi}_A$.

At $x = 0$, we use the following boundary condition for $\sqrt{\phi_A(x)}$

$$\frac{1}{\sqrt{\phi_A}} \frac{d\sqrt{\phi_A}}{dx}\bigg|_{x=0} = d^{-1} \quad (14)$$

We also use $(d\sqrt{\phi_A}/dx)|_{x=l} = 0$. The rest of the boundary conditions are the same as before; this gives $\omega_0 = \chi N(1 - 2\phi_{A,b}) - N \ln(1 - \phi_{A,b})$.

Our equations are identical to those used by Andelman and co-workers,[33-37] if we use $\rho_0 = a^{-3}$, $\chi = (1 - v\rho_0)/2$ (where v is the excluded-volume parameter used in their work), and the approximation

$$\ln \frac{1 - \phi_{A,b}}{1 - \phi_A(x)} \approx \phi_A(x) - \phi_{A,b}$$

The ODEs are solved by a relaxation method;[65] where a convergence criterion of 10^{-15} (defined in ref 65) is used. Again, we choose l to be large enough so that both $|\phi_A(l) - \phi_{A,b}|$ and $|\psi(l)|$ are less than 10^{-10}; this requires that L be from $84a$ to $2100a$ in our calculations, depending on the system parameters. Same as in the above full SCF calculations, the numerical accuracy is generally dictated by the discretization of the space domain. For cases of charged polymers, we extrapolate our numerical results to $m \to \infty$, based on the observation that all the calculated quantities are linear with l/m for $m \gtrsim 10^4$.[66] Once the SCF equations are solved, the mean-field free energy (of mixing) per polymer segment or solvent molecule can be calculated as (in units of k_BT)

$$f = \frac{1}{l}\int_0^l dx\left[\chi\phi_A{}^2(x) + \ln[1 - \phi_A(x)] - \frac{\epsilon}{2N}\left(\frac{d\psi}{dx}\right)^2\right] + \frac{\bar{\phi}_A\omega_0}{N} - \bar{\phi}_+ \ln\frac{Q_+}{\bar{\phi}_+} - \bar{\phi}_- \ln\frac{Q_-}{\bar{\phi}_-} \quad (15)$$

2.4. Calculated Quantities. In this work we focus on two calculated quantities: One is the amount of adsorbed polymers, $\Gamma \equiv \sqrt{N}\int_0^l dx\,[\phi_A(x) - \phi_{A,b}]$; polymers are depleted from the surface when $\Gamma < 0$, and adsorbed when $\Gamma > 0$. The other is the surface charge compensated by the adsorbed polymers, $\sigma \equiv \sigma_{SF} + v_A\sqrt{N}\int_0^l dx\,[p_A(x)\phi_A(x) - p\phi_{A,b}]$, where $p_A(x) \equiv -dg(x)/(v_A\,d\psi(x))$ is the local degree of ionization of the polymers; for charged surfaces, we have exact charge compensation when $\sigma = 0$, charge inversion when $\sigma < 0$, and full charge inversion when $r \equiv \sigma/\sigma_{SF} = -1$.[67]

For neutral polymers, eq 12 can be solved analytically under the approximation $\ln[(1 - \phi_{A,b})/(1 - \phi_A(x))] \approx \phi_A(x) - \phi_{A,b}$; for $l \to \infty$, this gives

$$\Gamma = \sqrt{\frac{(d^{-1})^2}{Nv^2} + \frac{2\phi_{A,b}}{v}} - \frac{d^{-1}}{\sqrt{N}v} - \sqrt{\frac{2\phi_{A,b}}{v}} \quad (16)$$

where $v \equiv 1 - 2\chi$ is the dimensionless excluded volume parameter. On the other hand, by integrating eq 4 with our boundary conditions, we get

$$\sigma = v_A p\phi_{A,b}\sqrt{N}\int_0^l dx\,[\exp(-v_+\psi) - 1] + v_+c_{s,b}\sqrt{N}\int_0^l dx\,[\exp(-v_-\psi) - \exp(-v_+\psi)]$$

Exact charge compensation is therefore always obtained when one sets both $\phi_{A,b} = 0$ and $c_{s,b} = 0$.

3. Numerical Results under GSDA

Hereafter, we only consider monovalent systems and set $v_A = v_- = -v_+ = -1$. In this section, we use the ground-state dominance approximation (GSDA) to explore the large parameter space involved in our model for flexible polyelectrolytes on flat surfaces, including the charge distribution of the polyelectrolytes (smeared vs annealed), degree of ionization of the polyelectrolytes p (varied from 0 to 1), surface charge density σ_{SF} (varied from 0 to 0.2), short-range (non-Coulombic) surface−polymer interactions characterized by d^{-1} (varied from −10 to ∞), solvent quality characterized by χ (varied from 0 to 1), bulk polymer segmental density $\phi_{A,b}$ (varied from 10^{-5} to 10^{-3}), and bulk salt concentration $c_{s,b}$ (varied from 0 to 0.1). For $a = 0.5$ nm and $\rho_0 = a^{-3}$, $\phi_{A,b} = 1.25 \times 10^{-4}$ corresponds to a bulk polymer segmental density of about 1.66 mM, $c_{s,b} = 0.1$ corresponds to a bulk salt concentration of about 1.33 M, and $\sigma_{SF} = 0.1$ corresponds to a surface charge density of about 2.61 ×

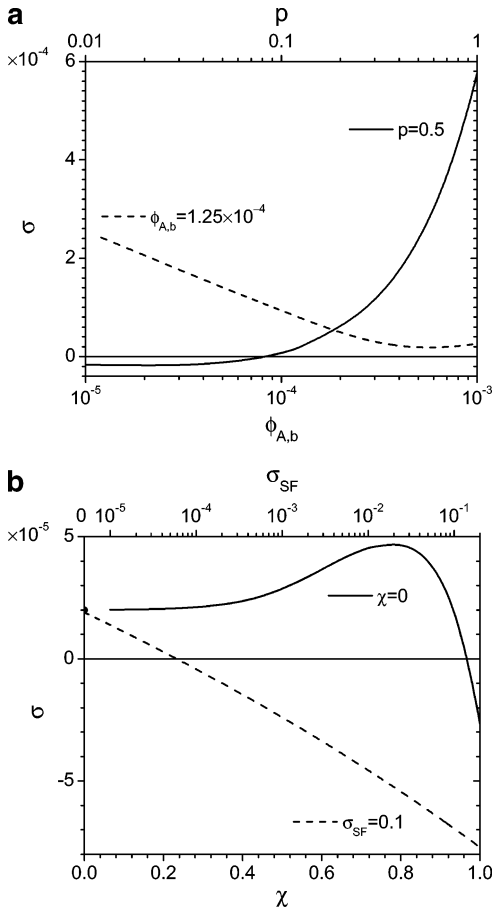

Figure 1. Effects of degree of ionization p, bulk polymer segmental density $\phi_{A,b}$, surface charge density σ_{SF}, and solvent quality χ on the surface charge compensation σ for nonadsorbing surfaces ($d^{-1} \to \infty$) in salt-free cases ($c_{s,b} = 0$). The results are obtained under the ground-state dominance approximation and for the smeared charge distribution. $\sigma_{SF} = 0.1$ and $\chi = 0$ in part a, and $p = 0.5$ and $\phi_{A,b} = 1.25 \times 10^{-4}$ in part b. The filled circle in part b corresponds to an uncharged surface ($\sigma_{SF} = 0$) in a good solvent ($\chi = 0$).

10^{-2} C/m^2. At $T = 300$ K, $\psi = 1$ corresponds to an electrostatic potential of about 25.9 mV. Under these conditions, a dielectric constant of 80 corresponds to $\epsilon \approx 0.343$ (which is used in this paper).

3.1. Nonadsorbing Surfaces. Here we set $d^{-1} \to \infty$. Figure 1 shows the effects of degree of ionization p, bulk polymer segmental density $\phi_{A,b}$, surface charge density σ_{SF}, and solvent quality χ on the surface charge compensation σ in salt-free cases for the smeared charge distribution. We see that σ in most cases is negligible compared to σ_{SF}, except when $\sigma_{SF} \lesssim 10^{-4}$ (where no charge inversion is obtained). Such small values of σ require accurate calculations of Γ (thus large values of m and l); in all of our numerical results, σ has at least three significant figures.

The almost exact charge compensation leads to $\Gamma \approx \sigma_{SF}/p$ for the smeared charge distribution where $p_A(x) = p$. This implies that $\phi_{A,b}$ and χ, the parameters representing short-range interactions in the system, have little effects on Γ when the electrostatic interactions dominate; this is supported by our data (not shown). The same conclusion can be drawn on the effects of d^{-1}, the parameter characterizing the short-range surface−polymer interactions (refer to Figure 6 below). As expected, for too small surface charge density ($\sigma_{SF} \lesssim 2 \times 10^{-5}$ for $p = 0.5$, $\phi_{A,b} = 1.25 \times 10^{-4}$, and $\chi = 0$), the

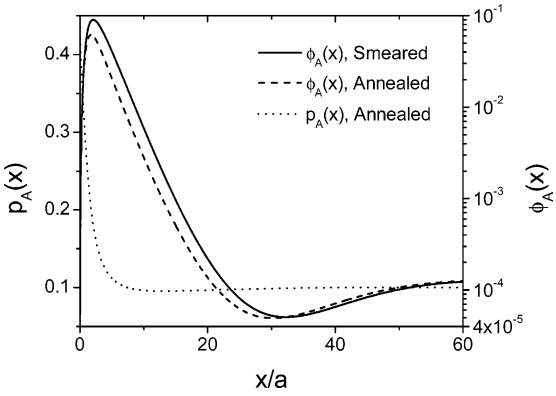

Figure 2. Comparison of polymer segmental density profiles $\phi_A(x)$ between the smeared and annealed charge distributions with the degree of ionization $p = 0.1$. Also shown is the local degree of ionization $p_A(x)$ for the annealed case. The results are obtained under the ground-state dominance approximation and for nonadsorbing surfaces ($d^{-1} \to \infty$), with $\sigma_{SF} = 0.1$, $c_{s,b} = 0$, $\chi = 0$, and $\phi_{A,b} = 1.25 \times 10^{-4}$.

effects of the infinitely large d^{-1} become dominant: polymers are depleted from the surface due to the loss of chain conformational entropy near the surface and Γ becomes negative.

The difference between the smeared and annealed charge distributions depends on both $\psi(x)$ and p; it diminishes when $\psi(x) = 0$, $p = 0$, or $p = 1$. In Figure 2, we compare the polymer segmental density profiles $\phi_A(x)$ for these two charge distributions, and also show the local degree of ionization $p_A(x)$ for the annealed case; other conditions ($\sigma_{SF} = 0.1$, $p = 0.1$, $c_{s,b} = 0$, $\chi = 0$, and $\phi_{A,b} = 1.25 \times 10^{-4}$) are the same for these two cases, which give $\psi_{SF} \approx 2.69$ in the smeared case and 1.88 in the annealed case. Here we see that polyelectrolytes in the annealed case carry much more charges in the vicinity of the surface but have smaller $\phi_A(x)$ from the surface to approximately the location of the first local minimum of $\phi_A(x)$. This gives no significant difference in the surface charge compensation: $\sigma \approx 9.34 \times 10^{-5}$ in the smeared case, and 4.68×10^{-5} in the annealed case. The difference between these two charge distributions becomes smaller for smaller $|\psi(x)|$ (e.g., as the bulk salt concentration $c_{s,b}$ increases). Hereafter, we focus on the smeared charge distribution, where the adsorbed amount and charge compensation are simply related through $\sigma = \sigma_{SF} - p\Gamma$.

The above results are for salt-free cases. Consistent with the previous numerical SCF study in continuum,[36] Γ decreases (σ increases) with increasing bulk salt concentration $c_{s,b}$ (not shown); i.e., we are in the screening-reduced regime.[14] At high enough $c_{s,b}$, electrostatic interactions are largely screened, and the polymers are depleted from the surface,[36] again due to the dominating effects of the infinitely large d^{-1}. For nonadsorbing surfaces, therefore, only slight charge inversion (if any) can be obtained.

3.2. Moderate Charge Inversion on Indifferent Surfaces in Θ-Solvent. Here we set $d^{-1} = 0$ and $\chi = {}^1/_2$. This case was studied analytically by Joanny, who predicted full charge inversion at high salt concentrations from the mean-field equations.[38] Figure 3 shows the effects of $c_{s,b}$, σ_{SF}, $\phi_{A,b}$, and p on the surface charge compensation σ. We do see that the charge inversion, or Γ equivalently, increases with increasing $c_{s,b}$, i.e., we are in the screening-enhanced regime;[14] but only moderate charge inversion ($-1 < \sigma/\sigma_{SF} < 0$) was obtained

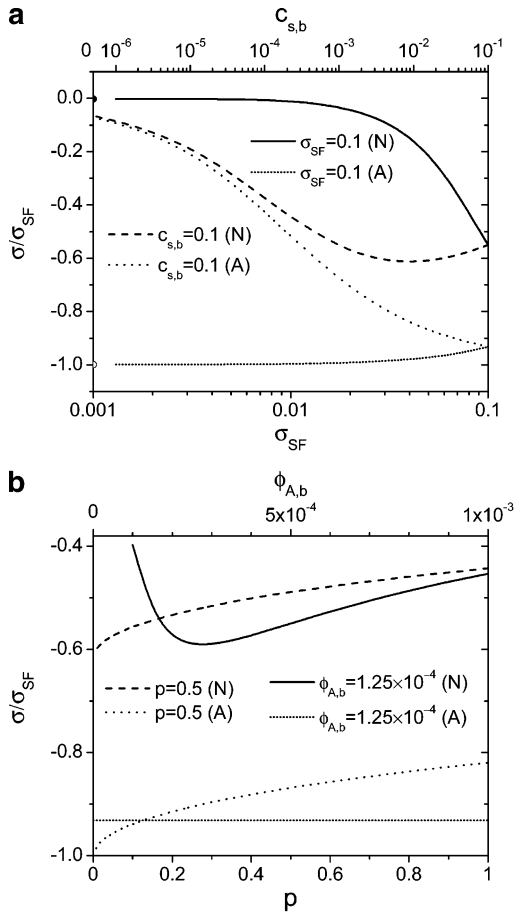

Figure 3. Effects of bulk salt concentration $c_{s,b}$, surface charge density σ_{SF}, bulk polymer segmental density $\phi_{A,b}$, and degree of ionization p on the surface charge compensation σ for indifferent surfaces ($d^{-1} = 0$) in Θ-solvent ($\chi = 1/2$). The results are obtained under the ground-state dominance approximation and for the smeared charge distribution. $p = 0.5$ and $\phi_{A,b} = 1.25 \times 10^{-4}$ in part a, and $\sigma_{SF} = 0.1$ and $c_{s,b} = 0.1$ in part b. Dotted curves are from the analytical theory, and the others are numerical results. The circles in part a correspond to salt-free cases ($c_{s,b} = 0$) with $\sigma_{SF} = 0.1$: the filled one is the numerical result and the open one is from the analytical theory. In part b, σ/σ_{SF} from the analytical theory for $\phi_{A,b} = 1.25 \times 10^{-4}$ slightly increases with decreasing p; while it should be 1 for neutral polymers ($p = 0$), the analytical theory gives a limit of about -0.9318 as $p \to 0$.

from the numerical results within reasonable parameter range. It is also interesting to see a minimum in σ/σ_{SF} as σ_{SF} or p varies.

Our results agree with the recent work by Shafir and Andelman, who numerically solved eqs 4 and 12 with $\phi_{A,b} = 0$ and Θ-solvent under the approximation $\ln[(1 - \phi_{A,b})/(1-\phi_A(x))] \approx \phi_A(x) - \phi_{A,b}$; they found only moderate charge inversion for attractive surfaces ($-6 \le d^{-1} \lesssim -0.462$) at high salt concentrations.[37] Under the same conditions, their charge inversion is only slightly larger than our results, since $\phi_A(x)$ is small in these calculations. A common problem associated with numerical calculations at $\phi_{A,b} \approx 0$ is demonstrated in Figure 4: even at a high salt concentration of $c_{s,b} = 0.1$, the decay of $\psi(x)$ to 0 becomes very slow as $\phi_{A,b}$ approaches 0; this requires large values of l in high-accuracy calculations. We therefore use 10^{-5} as the smallest $\phi_{A,b}$ in our calculations.

3.3. Strong Charge Inversion at High Salt Concentrations. The above results show that $\sigma \approx 0$ when the electrostatic interactions in the system dominate;

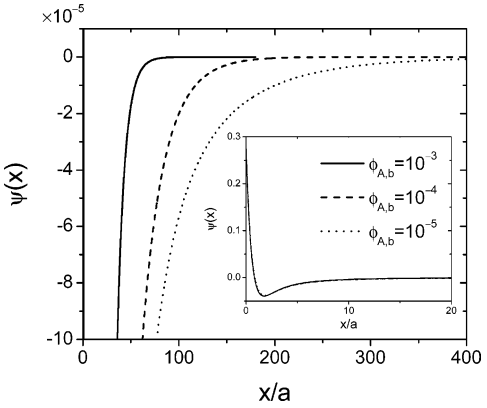

Figure 4. Decay of $\psi(x)$ to 0 becomes very slow as $\phi_{A,b}$ approaches 0. The results are obtained under the ground-state dominance approximation and for the smeared charge distribution, with $d^{-1} = 0$, $\sigma_{SF} = 0.1$, $p = 0.5$, $c_{s,b} = 0.1$, and $\chi = 1/2$. All curves virtually overlap in the inset.

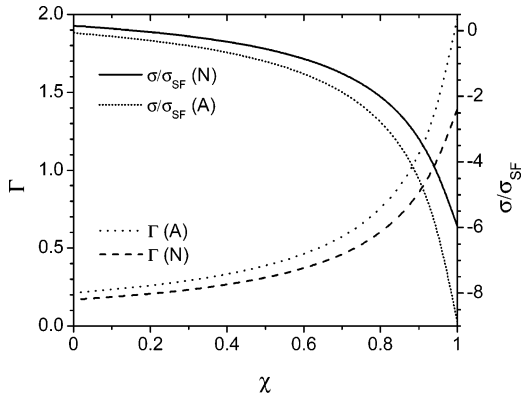

Figure 5. Effects of solvent quality χ on the amount of adsorbed polymers Γ and the surface charge compensation σ for an indifferent surface ($d^{-1} = 0$). The results are obtained under the ground-state dominance approximation and for the smeared charge distribution, with $\sigma_{SF} = 0.1$, $p = 0.5$, $c_{s,b} = 0.1$, and $\phi_{A,b} = 1.25 \times 10^{-4}$. Dotted curves are from the analytical theory, and the others are numerical results.

high salt concentrations are therefore necessary for obtaining at least moderate charge inversion (within the mean-field theory). Under such conditions, the solvent quality and short-range surface−polymer interactions also play important roles in obtaining strong charge inversion.

Figure 5 shows the effects of solvent quality, characterized by χ, on Γ and σ for an indifferent surface ($d^{-1} = 0$) at a high salt concentration ($c_{s,b} = 0.1$); almost 600% charge inversion is obtained at $\chi = 1$ from the numerical results! Note that this condition is not unusual because water is a poor solvent for hydrophobic polymer backbones. Such polyelectrolytes are water-soluble because of the large entropy gain of dissociated counterions and electrostatic interactions in the system, both of which are described by other terms in our theory, and not by the solvent quality characterized by the χ parameter. We note that poor solvent conditions have rarely been considered in previous mean-field studies on polyelectrolyte adsorption.[7,8,10,18,31,39]

The effects of the short-range surface−polymer interactions, characterized by d^{-1}, on Γ are shown in Figure 6. We see that d^{-1} has small or negligible effects when the electrostatic interactions in the system dominate, i.e., for polyelectrolytes in salt-free cases; this leads to $\sigma \approx 0$ and thus $\Gamma \approx \sigma_{SF}/p$ discussed above. However,

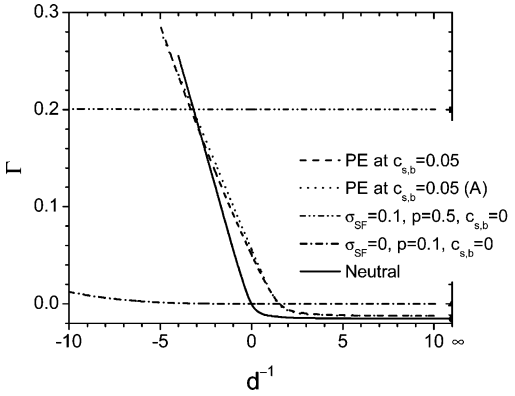

Figure 6. Effects of d^{-1}, the parameter characterizing the short-range surface−polymer interactions, on the amount of adsorbed polymers Γ. The results are obtained under the ground-state dominance approximation and for the smeared charge distribution. $\sigma_{SF} = 0.01$, $p = 0.5$, and $\chi = 1$ in the cases of polyelectrolytes (PE) at $c_{s,b} = 0.05$; $\chi = 0$ in all other cases; and $\phi_{A,b} = 1.25 \times 10^{-4}$ in all the cases. Dotted curve is from the analytical theory, and the others are numerical results. The filled symbols on the right axis are numerical results for nonadsorbing surfaces: the square is for the $\sigma_{SF} = 0.1$ and $p = 0.5$ case, the triangle is for the $\sigma_{SF} = 0$ and $p = 0.1$ case, the star is for the case of PE at $c_{s,b} = 0.05$, and the circle is for the neutral case (where $p = 0$ and $\sigma_{SF} = 0$).

d^{-1} has strong effects for polyelectrolytes at a high salt concentration ($c_{s,b} = 0.05$): $\sigma/\sigma_{SF} \approx -13.35$ at $d^{-1} = -5$. As shown in the figure, the adsorption behavior in this case is strikingly similar to that of neutral polymers in a good solvent ($\chi = 0$); this will be further investigated in section 4.

Figure 7 shows the effects of bulk polymer segmental density $\phi_{A,b}$, surface charge density σ_{SF}, bulk salt concentration $c_{s,b}$, and degree of ionization p on the surface charge compensation σ in a poor solvent ($\chi = 1$). Strong charge inversion ($\sigma/\sigma_{SF} < -1$) is found in most cases. Again, we see a minimum in σ/σ_{SF} as σ_{SF} varies. Note that in Figure 7b $p \gtrsim 0.316$ is needed in order to avoid (macroscopic) phase separation of the bulk solution; this is also required by the analytical theory, as discussed below.

4. Analytical Results at High Salt Concentrations

To better understand the adsorption behavior of polyelectrolytes at high salt concentrations, where moderate or strong charge inversion is found, we extend the work by Joanny, who analytically solved the mean-field equations at high salt concentrations with $\phi_{A,b} = 0$ and Θ-solvent under GSDA.[38] Here we consider only the smeared charge distribution and take $l \to \infty$. We assume $\ln[(1 - \phi_{A,b})/(1 - \phi_A(x))] \approx \phi_A(x) - \phi_{A,b}$, and $|\psi(x)| \ll 1$ at high salt concentrations. Under further approximations, the coupled ODEs, eqs 4 and 12, can be analytically solved (see Appendix for details, where the validity of these approximations are also examined); the final result is given by eq 16, with v and d^{-1} replaced by $v_{eff} \equiv v + p^2/c_b$ and $d_{eff}^{-1} \equiv d^{-1} - \sqrt{N}p\sigma_{SF}/c_b$, respectively, where $c_b \equiv p\phi_{A,b} + 2c_{s,b}$. We therefore see, at high salt concentrations, that charged polymers effectively increase the excluded volume parameter, and that a surface carrying opposite charges to the polyelectrolytes effectively makes the short-range surface−polymer interactions more attractive.

It is worth to note a few things about this analytical theory: First, when $\phi_{A,b} > 0$, Γ has the opposite sign to

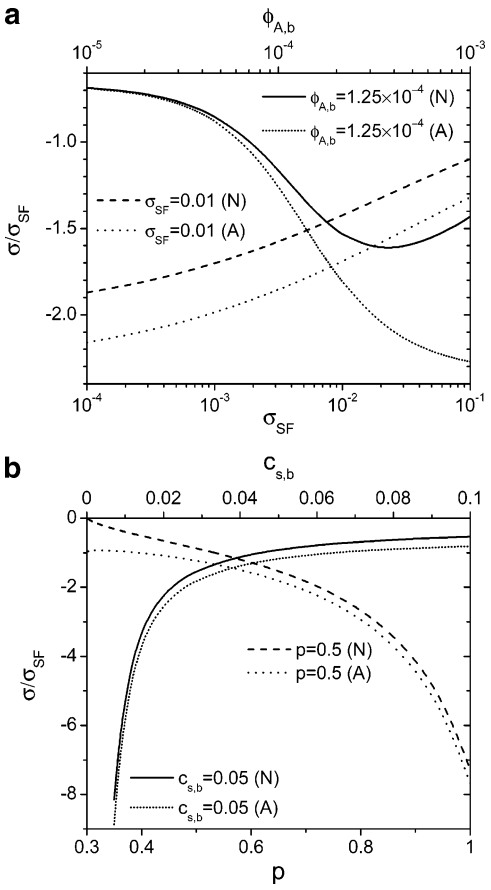

Figure 7. Effects of bulk polymer segmental density $\phi_{A,b}$, surface charge density σ_{SF}, bulk salt concentration $c_{s,b}$, and degree of ionization p on the surface charge compensation σ for indifferent surfaces ($d^{-1} = 0$) in a poor solvent ($\chi = 1$). The results are obtained under the ground-state dominance approximation and for the smeared charge distribution. $p = 0.5$ and $c_{s,b} = 0.05$ in part a, and $\sigma_{SF} = 0.01$ and $\phi_{A,b} = 1.25 \times 10^{-4}$ in part b. Dotted curves are from the analytical theory, and the others are numerical results.

d_{eff}^{-1}, as evident from eq 16; any charge inversion therefore requires $d_{eff}^{-1} < 0$. Second, the theory requires $v_{eff} > 0$, which leads to $p > \sqrt{v^2\phi_{A,b}^2/4 - 2vc_{s,b}} - v\phi_{A,b}/2$ when $v < 0$; this corresponds to $p \gtrsim 0.316$ in Figure 7b. Finally, for indifferent surfaces in Θ-solvent with any positive values of σ_{SF}, p, and $c_{s,b}$, the analytical theory predicts full charge inversion only when $\phi_{A,b} = 0$; any $\phi_{A,b} > 0$ will lead to less charge inversion.[68]

Predictions of the analytical theory are compared with numerical results in Figures 3, 5, 6, and 7; large deviations from the numerical results are seen in some cases, due to the approximations used in obtaining the analytical results (see Appendix). As expected, the analytical theory works better at higher salt concentrations; it also works better for smaller σ_{SF} and χ. Note that it is unable to capture the minima in σ/σ_{SF} revealed by numerical results. In all the cases, it overestimates the charge inversion, i.e., $\sigma^A < \sigma^N$ (when $\sigma^N < 0$), where the superscript "A" denotes the analytical results and "N" the numerical results. Since $(\sigma^A - \sigma^N)/\sigma^N = (\Gamma^A - \Gamma^N)/[\Gamma^N(1 - \sigma_{SF}/p\Gamma^N)]$, the analytical results have smaller relative error in the adsorbed amount than in the charge inversion when σ^N ($=\sigma_{SF} - p\Gamma^N$) < 0.

Although the analytical theory can only be used at small σ_{SF} ($\lesssim 0.01$), it qualitatively explains the mechanism of charge inversion at high salt concentrations, where the electrostatic interactions, although screened,

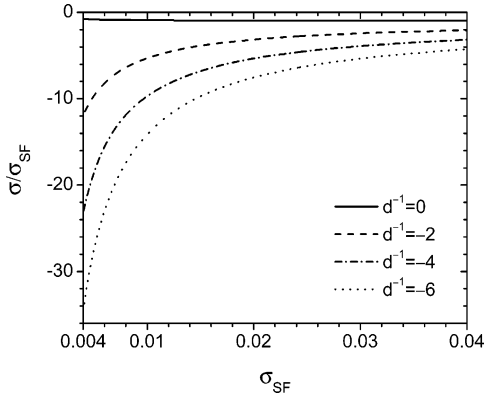

Figure 8. Qualitative comparison with Figure 6a in ref 19 on strong charge inversion for polyelectrolytes on attractive surfaces in Θ-solvent at a high salt concentration ($c_{s,b}$ = 0.1 M). The results are obtained using the analytical theory for p = 0.034 and $\phi_{A,b} = 5 \times 10^{-5}$. See text for details on the comparison.

still play important roles in the system. Taking as an example the polyelectrolytes ($p = 0.5$) on an oppositely charged ($\sigma_{SF} = 0.01$), indifferent ($d^{-1} = 0$) surface in a poor solvent ($v = -1$) at a high salt concentration ($c_{s,b} = 0.05$), if we ignore the small bulk polymer segmental density ($\phi_{A,b} = 0$), we obtain $v_{eff} = 1.5$ and $d_{eff}^{-1} = -0.05\sqrt{N}$. The strong charge inversion in this case, $\sigma/\sigma_{SF} \approx -2.333$, is therefore mainly due to the effectively attractive surface, i.e., the electrostatic contribution to d_{eff}^{-1}; the electrostatic contribution to v_{eff} in fact acts against the charge inversion (reduces Γ), and it is counteracted by the poor solvent to keep the charge inversion from being otherwise smaller. For quantitative comparison, if we use $\phi_{A,b} = 1.25 \times 10^{-4}$, eq 16 gives $\sigma/\sigma_{SF} \approx -1.810$, while the numerical solution under GSDA gives $\sigma/\sigma_{SF} \approx -1.534$ (shown later in Figure 10).

In Figure 8, we use the analytical theory to confirm the lattice SCF results of Shubin and Linse, who reported at high salt concentrations strong charge inversion for polyelectrolytes on attractive surfaces in Θ-solvent.[19] In their work, the polyelectrolytes consisted of neutral and charged (strongly dissociating) segments with the chain structure mapped from their experimental systems;[19] here we focus on the linear chain with the $p = 0.034$ case and use the smeared charge distribution instead. Since their chain length is large (N_A = 10 150), GSDA provides a good description in this case (refer to Figure 10 below). Their bulk salt concentration of 0.1 M corresponds to $c_{s,b} \approx 5.49 \times 10^{-3}$ here (with a = 0.45 nm used in their work and $\rho_0 = a^{-3}$), and we use $\phi_{A,b} = 5 \times 10^{-5}$ and Θ-solvent as in their work. Moreover, they used a charge-regulating surface whose charge density varies with solution pH, salt concentration, and the presence of polyelectrolytes; from Figure 2 of their paper, $\sigma_{SF} \approx 0.012$ C/m^2 (which corresponds to about 0.037 here) at pH = 6 and $c_{s,b}$ = 0.1 M with the polyelectrolytes adsorbed, and it decreases with decreasing pH, where charge inversion becomes stronger.[19] Here we use surfaces at constant charge density and vary σ_{SF} from 0.004 to 0.04. We also vary d^{-1} from 0 to −6; in their work the short-range surface−polymer attractions were characterized by a negative χ parameter between the surface and neutral polymer segments, and this is further complicated by the finite volume of ions who compete with polymers for surface adsorption. Despite all these differences, we see that the analytical theory well captures the strong charge inversion shown in Figure 6a of their paper. Note that it is essential to have an attractive surface in this case, since for indifferent surfaces in Θ-solvent only moderate charge inversion can be obtained, as shown in section 3.2.

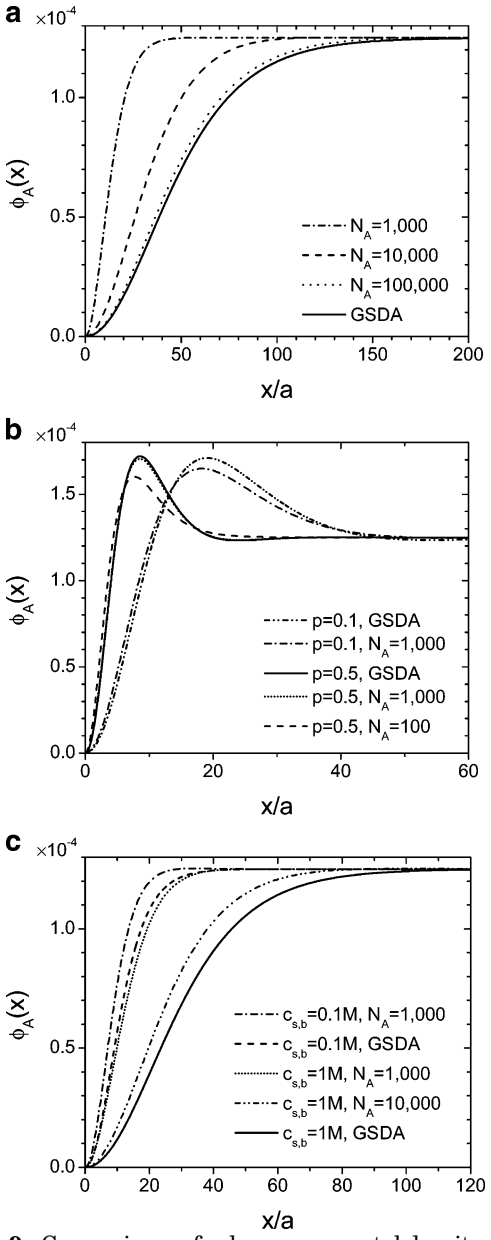

Figure 9. Comparisons of polymer segmental density profiles $\phi_A(x)$ from the ground-state dominance approximation with those from full self-consistent field calculations, for a uncharged, nonadsorbing surface ($\sigma_{SF} = 0$ and $d^{-1} \to \infty$) in a good solvent ($\chi = 0$). Key: (a) neutral polymers; (b) polyelectrolytes with no salt ($c_{s,b} = 0$); (c) polyelectrolytes ($p = 0.5$) with added salt, where the bulk salt concentrations are shown for $a = 0.5$ nm and $\rho_0 = a^{-3}$. Smeared charge distribution is used for polyelectrolytes, and $\phi_{A,b} = 1.25 \times 10^{-4}$ in all the cases.

5. Comparisons between SCF and GSDA Results

It is known that GSDA works better for polymers on surfaces or in confined geometries where the chains are in the "bound" state. Here we quantitatively assess the validity of GSDA by comparing its results with full SCF calculations. Since GSDA corresponds to $N_A \to \infty$, the comparison also reveals the effects of molecular weight of the polymers.

Figure 9 shows the polymer segmental density profiles on a uncharged, nonadsorbing surface ($\sigma_{SF} = 0$ and

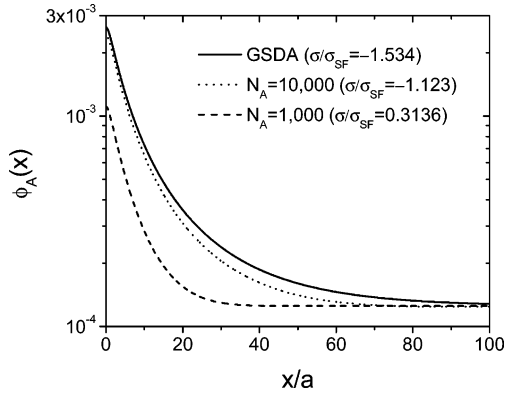

Figure 10. Comparison of polymer segmental density profiles $\phi_A(x)$ from the ground-state dominance approximation with those from full self-consistent field calculations, for a charged, indifferent surface ($\sigma_{SF} = 0.01$ and $d^{-1} = 0$) in a poor solvent ($\chi = 1$) at a high salt concentration ($c_{s,b} = 0.05$). Smeared charge distribution is used with $p = 0.5$, and $\phi_{A,b} = 1.25 \times 10^{-4}$.

$d^{-1} \to \infty$) in a good solvent ($\chi = 0$). We see that for neutral polymers GSDA is good only for rather long chains ($N_A \gtrsim 100\,000$). But it becomes much better for polyelectrolytes. For example, for the case of $N_A = 1000$ and $p = 0.5$ with no salt, the density profile from GSDA virtually overlaps with that from full SCF calculation, except around the peaks. This is due to the presence of counterions in the depletion zone right next to the surface, which attract polyelectrolytes to be closer to the surface than neutral polymers (as seen in the figure); this was examined in detail by Dahlgren and Leermakers using lattice SCF theory.[15] Even with added salt, which screens electrostatic interactions, the agreement between GSDA results and full SCF calculations are still improved relative to neutral cases. Note that the uncharged, nonadsorbing surface used here is the worst for polymer adsorption; the polymers are actually depleted ($\Gamma < 0$) in all the cases shown in Figure 9. For oppositely charged, less repulsive surfaces that favor the adsorption of polyelectrolytes, we would expect that, in most cases, GSDA results be in quantitative agreement with full SCF calculations. In other words, the molecular weight of the polyelectrolytes does not play a critical role here.

To check GSDA results on strong charge inversion, which are obtained at high salt concentrations, we compare in Figure 10 the polymer segmental density profiles on an oppositely charged, indifferent surface ($\sigma_{SF} = 0.01$ and $d^{-1} = 0$) in a poor solvent ($\chi = 1$) at a high salt concentration ($c_{s,b} = 0.05$). We see that the strong charge inversion is retained by relatively long chains ($N_A \gtrsim 10\,000$). Finally, since a poor solvent is used here, we check the possibility of (macroscopic) phase separation of the bulk solutions:[69] For $p = 0.5$ and $c_{s,b} = 0.05$, the smallest critical value of χ is 1.25, corresponding to $N_A \to \infty$, and it increases with decreasing N_A; the bulk solutions used in Figure 10 are therefore stable against (macroscopic) phase separation. We also used the random phase approximation[58] to check the possibility of microphase separation of the bulk solutions;[70] it cannot occur either in this case.

6. Conclusions

In this work, we have applied a continuum self-consistent field (SCF) theory to flexible polyelectrolytes on flat surfaces; the surface is either uncharged or carrying opposite charges to the polyelectrolytes. We examined in detail the effects of various parameters on the amount of polyelectrolyte adsorption (Γ) and surface charge compensation by the adsorbed polyelectrolytes (σ). The ground-state dominance approximation (GSDA) was used to explore the large parameter space involved, including the charge distribution and degree of ionization (p) of the polyelectrolytes, surface charge density (σ_{SF}), short-range (non-Coulombic) surface−polymer interactions (d^{-1}), solvent quality (χ), bulk polymer segmental density ($\phi_{A,b}$), and bulk salt concentration ($c_{s,b}$). The numerical results under GSDA were also compared with full SCF calculations to examine the effects of molecular weight of the polyelectrolytes. To better understand the adsorption behavior of polyelectrolytes at high salt concentrations, an analytical theory was developed and compared with numerical results under GSDA.

When the electrostatic interactions in the system dominate (e.g., when $c_{s,b}$ is small), only $\sigma \approx 0$ can be obtained, which leads to $\Gamma \approx \sigma_{SF}/p$ for the smeared charge distribution; parameters representing short-range interactions in the system (d^{-1}, χ, and $\phi_{A,b}$) have only small or negligible effects on Γ. Although the polymer segmental density profiles are different, both the smeared and annealed charge distributions give similar surface charge compensation.

At high salt concentrations, d^{-1} and χ play critical roles in determining the adsorption behavior of the system. For nonadsorbing surfaces ($d^{-1} \to \infty$), polymers are depleted due to the short-range repulsions between the surface and polymers. For indifferent surfaces ($d^{-1} = 0$) in Θ-solvent ($\chi = 1/2$), only moderate charge inversion ($-1 < \sigma/\sigma_{SF} < 0$) is found within reasonable parameter range. Strong charge inversion ($\sigma/\sigma_{SF} < -1$) is obtained by either decreasing d^{-1} (attractive surfaces) or increasing χ (poor solvent). The electrostatic interactions, although screened in this case, still play important roles in the system: charged polymers effectively increase the solvent quality (decrease χ), and a surface carrying opposite charges to the polyelectrolytes effectively makes the short-range surface−polymer interactions more attractive (decreases d^{-1}). The adsorption behavior of polyelectrolytes at high salt concentrations can therefore be understood by that of neutral polymers in good solvent, as shown by the analytical theory. The molecular weight plays minor role in polyelectrolyte adsorption even at high salt concentrations.

There are some limitations in this work: First, we ignored the volume and non-Coulombic interactions of small ions in the system. These ions compete with polymers for surface adsorption and could decrease the surface charge compensation by the polymers. Second, we used a uniform dielectric constant. Since the polymer concentration is low, the dielectric constant in the system can be approximated as uniform. However, the dielectric constant of the surface is in general much lower than that of water, and image charge effects[71−73] act against the adsorption of polyelectrolytes. Finally, since our study is at the mean-field level, we ignored correlations and fluctuations in the system, which have been shown to play important roles for polyelectrolytes on/between flat surfaces.[41−46,72−81] The necklace formation of polyelectrolytes in poor solvent and its influence on the adsorption are also not captured in our model. These could be topics for future publications.

Appendix

The starting point of the analytical theory is the following coupled ODEs

$$\frac{\epsilon}{N}\frac{d^2\psi}{dx^2} = (2c_{s,b} + p\phi_{A,b})\psi(x) + p(\phi_A(x) - \phi_{A,b}) \quad (17)$$

$$\frac{d^2}{dx^2}\sqrt{\phi_A} = N[v(\phi_A(x) - \phi_{A,b}) - p\psi(x)]\sqrt{\phi_A(x)} \quad (18)$$

with the boundary conditions $(d\psi/dx)|_{x=0} = -\sigma_{SF}\sqrt{N}/\epsilon$, $(d\psi/dx)|_{x\to\infty} = 0$, $(d\ \ln\sqrt{\phi_A}/dx)|_{x=0} = d^{-1}$, and $(d\sqrt{\phi_A}/dx)|_{x\to\infty} = 0$; we also have $\psi(x \to \infty) = 0$ and $\phi_A(x \to \infty) = \phi_{A,b}$. The exact analytical solution is unknown, and the analytical theory gives an approximate solution by decoupling the ODEs in a brute-force way. Mathematically, the analytical theory requires four approximations: First, $\phi_A(x)$ in eq 17 is constant; this gives

$$\psi(x) = \frac{\sigma_{SF}}{\sqrt{\epsilon c_b}}\exp\left(-x\sqrt{\frac{Nc_b}{\epsilon}}\right) - \frac{p}{c_b}(\phi_A(x) - \phi_{A,b}) \quad (19)$$

where $c_b \equiv p\phi_{A,b} + 2c_{s,b}$. Equation 18 then becomes

$$\frac{d^2}{dx^2}\sqrt{\phi_A} = Nv_{eff}(\phi_A(x) - \phi_{A,b})\sqrt{\phi_A(x)} - \frac{Np\sigma_{SF}}{\sqrt{\epsilon c_b}}\exp\left(-x\sqrt{\frac{Nc_b}{\epsilon}}\right)\sqrt{\phi_A(x)} \quad (20)$$

where $v_{eff} \equiv v + p^2/c_b$. Again, its exact analytical solution (for $x \in [0, \infty)$) is unknown. Instead, we solve it in the interval $[h,\infty)$ (where $h > 0$) by ignoring its last term; this requires the second approximation, $\exp(-h\sqrt{Nc_b/\epsilon}) \approx 0$. In addition, a boundary condition for $\sqrt{\phi_A(x)}$ at $x = h$ is needed; this is obtained by integrating $d(d(\ln\sqrt{\phi_A})/dx) = [(d^2\sqrt{\phi_A}/d^2x)/\sqrt{\phi_A} - (d(\ln\sqrt{\phi_A})/dx)^2]dx$ from $x = 0$ to h using eq 20, which gives

$$\frac{1}{\sqrt{\phi_A}}\frac{d\sqrt{\phi_A}}{dx}\bigg|_{x=h} = d_{eff}^{-1} + \Delta$$

where $d_{eff}^{-1} \equiv d^{-1} - \sqrt{N}p\sigma_{SF}/c_b$ and $\Delta \equiv \int_0^h dx[Nv_{eff}(\phi_A - \phi_{A,b}) - (d\sqrt{\phi_A}/dx)^2/\phi_A] + (\sqrt{N}p\sigma_{SF}/c_b)\exp(-h\sqrt{Nc_b/\epsilon})$. With the third approximation, $\int_0^h dx\,[Nv_{eff}(\phi_A - \phi_{A,b}) - (d\sqrt{\phi_A}/dx)^2/\phi_A] \approx 0$ for small h, the problem can then be solved analytically, in analogy to the adsorption of neutral polymers in a good solvent. Finally, we need the fourth approximation, which changes the lower integration limit for Γ from 0 to h; the final result for Γ is given by eq 16, with v and d^{-1} replaced by v_{eff} and d_{eff}^{-1}, respectively (this is the analytical results plotted in all the figures).

The polymer segmental density at the surface, which is approximated by that at $x = h$ from the analytical theory, is given by

$$\phi_{A,SF} = \phi_{A,b} + \frac{(d_{eff}^{-1})^2}{Nv_{eff}} - \frac{d_{eff}^{-1}}{Nv_{eff}}\sqrt{(d_{eff}^{-1})^2 + 2Nv_{eff}\phi_{A,b}}$$

and ψ_{SF} can be obtained by substituting the above result into eq 19. These results, as well as that for Γ, can be further simplified in two limits: When $(d_{eff}^{-1})^2 \gg 2Nv_{eff}\phi_{A,b}$, they become

$$\begin{cases} \Gamma \approx -\sqrt{\dfrac{2\phi_{A,b}}{v_{eff}}} \\ \phi_{A,SF} \approx \dfrac{Nv_{eff}}{2(d_{eff}^{-1})^2}\phi_{A,b}^{\ 2} \quad \text{for } d_{eff}^{-1} > 0, \text{ and} \\ \psi_{SF} \approx \dfrac{\sigma_{SF}}{\sqrt{\epsilon c_b}} + \dfrac{p}{c_b}\phi_{A,b} \end{cases}$$

$$\begin{cases} \Gamma \approx -\dfrac{2d_{eff}^{-1}}{\sqrt{N}v_{eff}} \\ \phi_{A,SF} \approx \dfrac{2(d_{eff}^{-1})^2}{Nv_{eff}} \quad \text{for } d_{eff}^{-1} < 0 \quad (21) \\ \psi_{SF} \approx \dfrac{\sigma_{SF}}{\epsilon c_b} - \dfrac{2(d_{eff}^{-1})^2}{Nv_{eff}}\dfrac{p}{c_b} \end{cases}$$

when $(d_{eff}^{-1})^2 \ll 2Nv_{eff}\phi_{A,b}$, they become

$$\begin{cases} \Gamma \approx -\dfrac{d_{eff}^{-1}}{\sqrt{N}v_{eff}} + \dfrac{(d_{eff}^{-1})^2}{\sqrt{8\phi_{A,b}}Nv_{eff}^{3/2}} \\ \phi_{A,SF} \approx \phi_{A,b} - d_{eff}^{-1}\sqrt{\dfrac{2\phi_{A,b}}{Nv_{eff}}} \\ \psi_{SF} \approx \dfrac{\sigma_{SF}}{\sqrt{\epsilon c_b}} + d_{eff}^{-1}\sqrt{\dfrac{2\phi_{A,b}}{Nv_{eff}}}\dfrac{p}{c_b} \end{cases}$$

The above four approximations used to derive the analytical theory are "uncontrolled"; while the second approximation favors a large h and the last two favor a small h, the first approximation is probably the most problematic (it is obviously not satisfied by the analytical solution). Physically, this approximation corresponds to the case where the decay of $\psi(x)$ is much faster than that of $\phi_A(x)$, as pointed out by Joanny.[38] From Figure 11, which shows the numerical solutions to eqs 4 and 12 (strictly speaking, to examine the validity of the first approximation, one should numerically solve eqs 17 and 18, but the differences caused by the approximations $\ln[(1 - \phi_{A,b})/(1 - \phi_A(x))] \approx \phi_A(x) - \phi_{A,b}$ and $|\psi(x)| \ll 1$ should be negligible in these cases), we see that this is the case at high salt concentrations (note the different scales of horizontal axes). $\phi_A(x)$, however, is certainly not constant near the surface (note the logarithmic scale for $\phi_A(x)$) unless both $d^{-1} = 0$ and $\sigma_{SF} = 0$; since solving eq 17 requires integration over the entire range of x, this is probably the major source of error for the analytical theory at large σ_{SF}, where the variation of $\phi_A(x)$ near the surface becomes sharp.

To examine the second and third approximations, we numerically solve eq 20 using the relaxation method[65] (where $L = 420a$ and $m = 1.4 \times 10^6$ are used). Figure 12 shows the values of h (which minimizes Δ) and the corresponding Δ (divided by $-d_{eff}^{-1}$, which is positive in these calculations) as a function of σ_{SF}. We see that Δ becomes comparable to $-d_{eff}^{-1}$ at large σ_{SF}; this is also responsible for the large deviations seen in such cases.

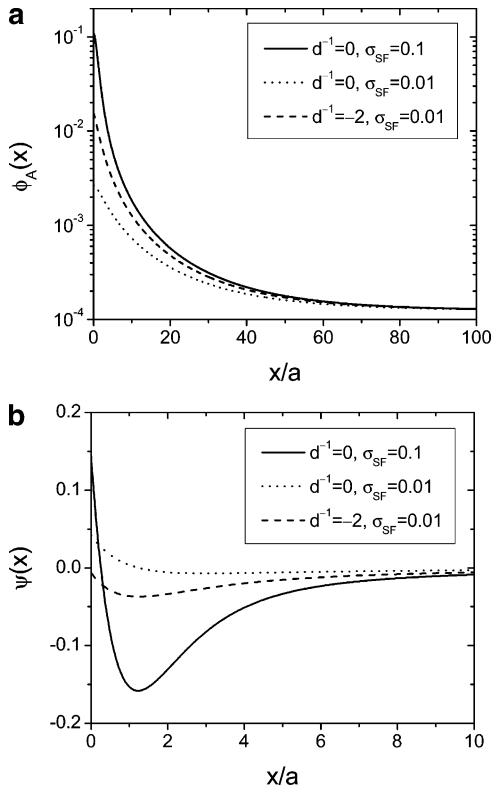

Figure 11. (a) Polymer segmental density profile $\phi_A(x)$, and (b) electrostatic potential $\psi(x)$. The results are obtained under the ground-state dominance approximation and for the smeared charge distribution, with $p = 0.5$, $c_{s,b} = 0.05$, $\chi = 1$, and $\phi_{A,b} = 1.25 \times 10^{-4}$.

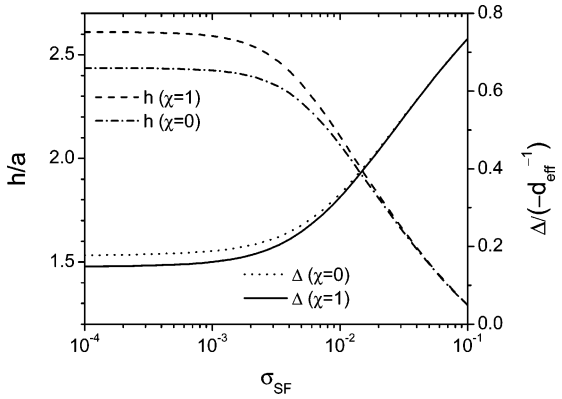

Figure 12. Values of h (which minimizes Δ) and the corresponding Δ as a function of σ_{SF}. The results are obtained from the numerical solution to eq 20, with $d^{-1} = 0$, $p = 0.5$, $c_{s,b} = 0.05$, and $\phi_{A,b} = 1.25 \times 10^{-4}$. Note that $d_{eff}^{-1} < 0$ in these calculations.

We also see that h is indeed small, which favors the fourth approximation.

Acknowledgment. The author thanks Adi Shafir and Prof. David Andelman for helpful discussions and for their preprint of ref 37 before its publication. Financial support for this work was provided by Colorado State University, which is gratefully acknowledged.

References and Notes

(1) Fleer, G. J.; Cohen Stuart, M. A.; Scheutjens, J. M. H. M.; Cosgrove, T.; Vincent, B. *Polymers at Interfaces*; Cambridge University Press: Cambridge, U.K., 1993.
(2) Netz, R. R.; Andelman, D. *Phys. Rep.* **2003**, *380*, 1.
(3) Hesselink, F. Th. *J. Electroanal. Chem.* **1972**, *37*, 317.
(4) Hesselink, F. Th. *J. Colloid Interface Sci.* **1977**, *60*, 448.
(5) Scheutjens, J. M. H. M.; Fleer, G. J. *J. Phys. Chem.* **1979**, *83*, 1619.
(6) Scheutjens, J. M. H. M.; Fleer, G. J. *J. Phys. Chem.* **1980**, *84*, 178.
(7) van der Schee, H. A.; Lyklema, J. *J. Phys. Chem.* **1984**, *88*, 6661.
(8) Papenhuijzen, J.; van der Schee, H. A.; Fleer, G. J. *J. Colloid Interface Sci.* **1985**, *104*, 540.
(9) Roe, R. J. *J. Chem. Phys.* **1974**, *60*, 4192.
(10) Evers, O. A.; Fleer, G. J.; Scheutjens, J. M. H. M.; Lyklema, J. *J. Colloid Interface Sci.* **1986**, *111*, 446.
(11) Bohmer, M. R.; Evers, O. A.; Scheutjens, J. M. H. M. *Macromolecules* **1990**, *23*, 2288.
(12) Scheutjens, J. M. H. M.; Fleer, G. J. *Macromolecules* **1985**, *18*, 1882.
(13) Fleer, G. J.; Scheutjens, J. M. H. M. *J. Colloid Interface Sci.* **1986**, *111*, 504.
(14) van de Steeg, H. G. M.; Stuart, M. A. C.; de Keizer, A.; Bijsterbosch, B. H. *Langmuir* **1992**, *8*, 2538.
(15) Dahlgren, M. A. G.; Leermakers, F. A. M. *Langmuir* **1995**, *11*, 2996.
(16) Linse, P. *Macromolecules* **1996**, *29*, 326.
(17) Fleer, G. J. *Ber. Bunsen-Ges. Phys. Chem.* **1996**, *100*, 936.
(18) Vermeer, A. W. P.; Leermakers, F. A. M.; Koopal, L. K. *Langmuir* **1997**, *13*, 4413.
(19) Shubin, V.; Linse, P. *Macromolecules* **1997**, *30*, 5944.
(20) Wiegel, F. W. *J. Phys. A: Math. Gen.* **1977**, *10*, 299.
(21) Gaylord, R. J.; Zhang, H. *J. Chem. Phys.* **1987**, *86*, 440.
(22) Muthukumar, M. *J. Chem. Phys.* **1987**, *86*, 7230.
(23) van Opheusden, J. H. J. *J. Phys. A: Math. Gen.* **1988**, *21*, 2739.
(24) Podgornik, R. *Chem. Phys. Lett.* **1990**, *174*, 191.
(25) Podgornik, R. *J. Phys. Chem.* **1991**, *95*, 5249.
(26) Podgornik, R. *J. Phys. Chem.* **1992**, *96*, 884.
(27) Podgornik, R. *Croat. Chem. Acta* **1992**, *65*, 285.
(28) Varoqui, R.; Johner, A.; Elaissari, A. *J. Chem. Phys.* **1991**, *94*, 6873.
(29) Varoqui, R. *J. Phys. II* **1993**, *3*, 1097.
(30) Varoqui, R. *ACS Symp. Ser.* **1994**, *548*, 421.
(31) Chatellier, X.; Joanny, J. F. *J. Phys. II* **1996**, *6*, 1669.
(32) Solis, F. J.; de la Cruz, M. O. *J. Chem. Phys.* **1999**, *110*, 11517.
(33) Borukhov, I.; Andelman, D.; Orland, H. *Europhys. Lett.* **1995**, *32*, 499.
(34) Borukhov, I.; Andelman, D.; Orland, H. *Macromolecules* **1998**, *31*, 1665.
(35) Borukhov, I.; Andelman, D.; Orland, H. *J. Phys. Chem. B* **1999**, *103*, 5042.
(36) Shafir, A.; Andelman, D.; Netz, R. R. *J. Chem. Phys.* **2003**, *119*, 2355.
(37) Shafir, A.; Andelman, D. *Phys. Rev. E* **2004**, *70*, 061804.
(38) Joanny, J. F. *Eur. Phys. J. B* **1999**, *9*, 117.
(39) Dobrynin, A. V. *J. Chem. Phys.* **2001**, *114*, 8145.
(40) Huang, H.; Ruckenstein, E. *Adv. Colloid Interface Sci.* **2004**, *112*, 37.
(41) Dobrynin, A. V.; Deshkovski, A.; Rubinstein, M. *Macromolecules* **2001**, *34*, 3421.
(42) Dobrynin, A. V.; Rubinstein, M. *Macromolecules* **2002**, *35*, 2754.
(43) Dobrynin, A. V.; Rubinstein, M. *J. Phys. Chem. B* **2003**, *107*, 8260.
(44) Chang, R.; Yethiraj, A. *Prog. Org. Coat.* **2003**, *47*, 331.
(45) Patra, C. N.; Chang, R.; Yethiraj, A. *J. Phys. Chem. B* **2004**, *108*, 9126.
(46) Messina, R. *Macromolecules* **2004**, *37*, 621.
(47) Decher, G. *Science* **1997**, *277*, 1232.
(48) Bertrand, P.; Jonas, A.; Laschewsky, A.; Legras, R. *Macromol. Rapid Commun.* **2000**, *21*, 319.
(49) Schonhoff, M. *J. Phys.: Condens. Matter* **2003**, *15*, R1781.
(50) Afsharrad, T.; Bailey, A. I.; Luckham, P. F.; Macnaughtan, W.; Chapman, D. *Colloids Surf.* **1987**, *25*, 263.
(51) Tanaka, H.; Odberg, L.; Wagberg, L.; Lindstrom, T. *J. Colloid Interface Sci.* **1990**, *134*, 219.
(52) Berndt, P.; Kurihara, K.; Kunitake, T. *Langmuir* **1992**, *8*, 2486.
(53) Eriksson, L.; Alm, B.; Stenius, P. *Colloids Surf. A* **1993**, *70*, 47.
(54) Dahlgren, M. A. G.; Claesson, P. M.; Audebert, R. *J. Colloid Interface Sci.* **1994**, *166*, 343.
(55) Shubin, V.; Samoshina, Y.; Menshikova, A.; Evseeva, T. *Colloid Polym. Sci.* **1997**, *275*, 655.
(56) Shubin, V. *J. Colloid Interface Sci.* **1997**, *191*, 372.

(57) Shi, A. C.; Noolandi, J. *Macromol. Theory Simul.* **1999**, *8*, 214.
(58) Wang, Q.; Taniguchi, T.; Fredrickson, G. H. *J. Phys. Chem. B* **2004**, *108*, 6733, **2005**, *109*, 9855.
(59) For nonadsorbing surfaces the initial condition for q becomes $q(x > 0, s = 0) = 1$, while $q(x \geq 0, s = 0) = 1$ is applied in all other cases.
(60) Mitchell, A. R.; Griffiths, D. F. *The Finite Difference Method in Partial Differential Equations*; John Wiley & Sons, Inc.: New York, 1980; Chapter 2.4.
(61) Tzeremes, G.; Rasmussen, K. O.; Lookman, T.; Saxena, A. *Phys. Rev. E* **2002**, *65*, 041806.
(62) $\omega_A(x_0)$ and $F_1(x_0)$ are not needed for nonadsorbing surfaces.
(63) Press, W. H.; Teukolsky, S. A.; Vetterling, W. T.; Flannery, B. P. *Numerical Recipes in C: the Art of Scientific Computing*, 2nd ed.; Cambridge University Press: Cambridge, U.K., 2002; Chapter 9.7.
(64) de Gennes, P. G. *Scaling Concepts in Polymer Physics*; Cornell University Press: Ithaca, NY, 1979.
(65) Press, W. H.; Teukolsky, S. A.; Vetterling, W. T.; Flannery, B. P. *Numerical Recipes in C: the Art of Scientific Computing*, 2nd ed.; Cambridge University Press: Cambridge, U.K., 2002; Chapter 17.3.
(66) In particular, the integrated total charge density in the system (including the surface charges) is inversely proportional to m; we use this to choose the values of m ($>10^5$) in the extrapolation.
(67) In some studies, the charge inversion is identified by an extremum in $\psi(x)$; the integrated total charge from the surface to the location of the extremum (including the surface charges) is 0. Since the charges carried by small ions are also included in this integration, it is different from what we consider here: in our calculations of σ, we take into account only the charges carried by the polymers.
(68) This follows directly from the inequality $\sqrt{b^2+c^2} \leq b + c$ (for $b > 0$ and $c \geq 0$), where the equal sign is taken only when $c = 0$; here $b \equiv -d_{\text{eff}}^{-1}/(\sqrt{N}v_{\text{eff}}) = \sigma_{\text{SF}}/p > 0$, and $c \equiv \sqrt{2\phi_{A,b}/v_{\text{eff}}}$.
(69) Warren, P. B. *J. Phys. II* **1997**, *7*, 343.
(70) Boryu, V. Yu.; Erukhimovich, I. Ya. *Sov. Phys. Dokl.* **1986**, *31*, 146.
(71) Netz, R. R.; Joanny, J. F. *Macromolecules* **1999**, *32*, 9013.
(72) Messina, R. *Phys. Rev. E* **2004**, *70*, 051802.
(73) Cheng, C.-H.; Lai, P. Y. *Phys. Rev. E* **2004**, *70*, 061805.
(74) Akesson, T.; Woodward, C.; Jonsson, B. *J. Chem. Phys.* **1989**, *91*, 2461.
(75) Beltran, S.; Hooper, H. H.; Blanch, H. W.; Prausnitz, J. M. *Macromolecules* **1991**, *24*, 3178.
(76) Kong, C. Y.; Muthukumar, M. *J. Chem. Phys.* **1998**, *109*, 1522.
(77) Carignano, M. A.; Dan, N. *Langmuir* **1998**, *14*, 3475.
(78) Yethiraj, A. *J. Chem. Phys.* **1999**, *111*, 1797.
(79) Dobrynin, A. V.; Deshkovski, A.; Rubinstein, M. *Phys. Rev. Lett.* **2000**, *84*, 3101.
(80) Podgornik, R.; Dobnikar, J. *J. Chem. Phys.* **2001**, *115*, 1951.
(81) Jonsson, B.; Broukhno, A.; Forsman, J.; Akesson, T. *Langmuir* **2003**, *19*, 9914.

MA050960B